THE JOURNAL OF BIOLOGICAL CHEMISTRY VOL. 287, NO. 52, pp. 43401–43409, December 21, 2012

Foamy Virus Envelope Protein Is a Substrate for Signal Peptide Peptidase-like 3 (SPPL3)*[S]

Received for publication, April 11, 2012, and in revised form, October 26, 2012 Published, JBC Papers in Press, November 6, 2012, DOI 10.1074/jbc.M112.371369

Matthias Voss[‡1], Akio Fukumori[‡], Peer-Hendrik Kuhn[§], Ulrike Künzel[‡], Bärbel Klier[‡], Gudula Grammer[‡], Martina Haug-Kröper[‡], Elisabeth Kremmer[§¶], Stefan F. Lichtenthaler[§‖], Harald Steiner[‡§], Bernd Schröder[‡‡], Christian Haass[‡§‖2], and Regina Fluhrer[‡§3]**

From the [‡]Adolf Butenandt Institute for Biochemistry, Ludwig-Maximilians University Munich, the [§]German Center for Neurodegenerative Diseases (DZNE), and the [‖]Munich Cluster for Systems Neurology (SyNergy), 80336 Munich, Germany, the [¶]Institute of Molecular Immunology, Helmholtz Zentrum München, German Research Center for Environmental Health and [**]Technische Universität München, 81377 Munich, Germany, and the [‡‡]Biochemical Institute, Christian-Albrechts University Kiel, 24118 Kiel, Germany

Background: SPPL proteases are intramembrane-cleaving aspartyl proteases of the G*x*GD type.
Results: Under certain circumstances, SPPL3 cleaves FVenv independent of prior shedding, generating substrates for subsequent intramembrane proteolysis.
Conclusion: Unlike other known G*x*GD proteases, SPPL3 can act as a sheddase and an intramembrane protease within the regulated intramembrane proteolysis cascade.
Significance: This initial biochemical characterization of SPPL3 will help to address its physiological role in later studies.

Signal peptide peptidase (SPP), its homologs, the SPP-like proteases SPPL2a/b/c and SPPL3, as well as presenilin, the catalytic subunit of the γ-secretase complex, are intramembrane-cleaving aspartyl proteases of the G*x*GD type. In this study, we identified the 18-kDa leader peptide (LP18) of the foamy virus envelope protein (FVenv) as a new substrate for intramembrane proteolysis by human SPPL3 and SPPL2a/b. In contrast to SPPL2a/b and γ-secretase, which require substrates with an ectodomain shorter than 60 amino acids for efficient intramembrane proteolysis, SPPL3 cleaves mutant FVenv lacking the proprotein convertase cleavage site necessary for the prior shedding. Moreover, the cleavage product of FVenv generated by SPPL3 serves as a new substrate for consecutive intramembrane cleavage by SPPL2a/b. Thus, human SPPL3 is the first G*x*GD-type aspartyl protease shown to be capable of acting like a sheddase, similar to members of the rhomboid family, which belong to the class of intramembrane-cleaving serine proteases.

Regulated intramembrane proteolysis describes a two-step proteolytic processing pathway required for protein degradation and cellular signaling of many membrane proteins (1). Typically, regulated intramembrane proteolysis substrates are first cleaved within their luminal domain to release a large part of their ectodomain or to clip a hairpin loop between two transmembrane domains (TMDs).[4] This cleavage is termed "shedding" and generates a membrane-retained fragment, which is subsequently processed by an intramembrane-cleaving protease (2–4). Intramembrane proteases are defined as proteolytic enzymes "which reside within cellular membranes and their active sites are buried within the TMD, where they cleave in, or immediately adjacent to, transmembrane domains of their substrates, thereby releasing soluble domains from membrane proteins" (5). So far, intramembrane aspartyl, serine, and metalloproteases have been described (4). Intramembrane-cleaving proteases of the aspartyl protease class are G*x*GD proteases (2, 3). G*x*GD describes the amino acid motif in TMD7 of the unconventional but highly conserved protease active site (6). In humans, two subfamilies of G*x*GD proteases are known: presenilin-1 and presenilin-2, which constitute the catalytic subunit of the γ-secretase complex, and signal peptide peptidase (SPP) and its homologs, the SPP-like (SPPL) proteases SPPL2a/b/c and SPPL3 (3). All known γ-secretase substrates are type I transmembrane proteins (2), whereas SPP/SPPLs selectively cleave type II transmembrane proteins (3). This is consistent with the opposite orientation of the catalytic sites of presenilin and SPP/SPPLs (7). One common requirement for substrate recognition by γ-secretase, SPP, and SPPL2a/b is truncation of the corresponding substrate by shedding, which always precedes intramembrane proteolysis and generates integral membrane proteins short enough to be recognized by these proteases (8–10).

* This work was supported in part by Deutsche Forschungsgemeinschaft Grant HA 1737-11 (to R. F. and C. H.) and the Competence Network for Neurodegenerative Diseases (KNDD) of the Bundesministerium für Bildung und Forschung.
[S] This article contains supplemental Figs. S1 and S2.
[1] Supported by a Ph.D. fellowship from the Hans und Ilse Breuer Stiftung and by the Elitenetwork of Bavaria within the Graduate Program "Protein Dynamics in Health and Disease."
[2] Member of the Center for Integrated Protein Science Munich (CIPS[M]). Supported by a "Forschungsprofessur" from the Ludwig-Maximilians University.
[3] To whom correspondence should be addressed: Adolf Butenandt Institute for Biochemistry, Ludwig-Maximilians University Munich and DZNE, Schillerstr. 44, D-80336 Munich, Germany. Tel.: 49-89-2180-75487; Fax: 49-89-2180-75415; E-mail: regina.fluhrer@dzne.lmu.de.

[4] The abbreviations used are: TMD, transmembrane domain; SPP, signal peptide peptidase; SPPL, SPP-like; FVenv, foamy virus envelope protein; $(Z\text{-}LL)_2$ ketone,1,3-di-(*N*-benzyloxycarbonyl-L-leucyl-L-leucyl)aminoacetone; DAPT, *N*-[*N*-(3,5-difluorophenacetyl)-L-alanyl]-*S*-phenylglycine *t*-butyl ester; ER, endoplasmic reticulum; PC, proprotein convertase; Tricine, *N*-[2-hydroxy-1,1-bis(hydroxymethyl)ethyl]glycine.

Because only artificial model substrates optimized for SPP cleavage have been used so far to study the proteolytic activity of human SPPL3 (11), very little is known about its biochemical properties. We noticed that, compared with other retroviral signal or leader peptides, the foamy virus envelope (FVenv) protein harbors an unusually long leader peptide (LP18, $gp18^{LP}$) that is stably integrated into mature virus particles as a type II-oriented transmembrane protein (12). Interestingly, budding of foamy virus particles is observed at intracellular membranes (12). On the basis of this knowledge and our previous observation that individual members of the SPP/SPPL family reside within early secretory compartments (3), we speculated that LP18 of FVenv might be a substrate for SPP/SPPL proteases.

Indeed, we found that the FVenv protein undergoes intramembrane proteolysis mediated by SPPL3 and, in addition, by SPPL2a/b. In contrast to intramembrane proteolysis by SPPL2a/b, cleavage of FVenv by SPPL3 is not dependent on the size of the substrate's ectodomain and is, surprisingly, not sensitive to treatment with known G*x*GD protease inhibitors. In addition, the cleavage product of LP18 generated by SPPL3 cleavage constitutes a substrate for consecutive intramembrane cleavage by SPPL2a/b.

EXPERIMENTAL PROCEDURES

Antibodies and Reagents—Monoclonal antibodies against SPPL2a and SPPL3 were produced by immunization with synthetic peptides. 2a01 6E9 (mouse IgG1) was generated against peptides comprising amino acids 199–217 of human SPPL2a, and L302 7F9 (mouse IgG1) against amino acids 247–261 of human SPPL3. Anti-FLAG monoclonal (M2) and polyclonal antibodies and anti-FLAG M2-agarose conjugates were obtained from Sigma-Aldrich. Other antibodies used were anti-V5 polyclonal antibody (Millipore), anti-KDEL and anti-calnexin polyclonal antibodies (Enzo Life Sciences), anti-V5 monoclonal antibody (Invitrogen), anti-HA antibody 3F10 (Roche Diagnostics), and anti-HA polyclonal and anti-actin monoclonal antibodies (Sigma-Aldrich). The SPPL2b-specific monoclonal antibody CADG-3F9 has been described previously (13). $(Z\text{-}LL)_2$ ketone and L-685,458 were obtained from Calbiochem, and *N*-[*N*-(3,5-difluorophenacetyl)-L-alanyl]-*S*-phenylglycine *t*-butyl ester (DAPT) was from Enzo Life Sciences. Inhibitor treatment was carried out for 16 h.

Expression Constructs, Cell Lines, and Transfections—SFVcpz(hu) coding sequences were amplified by PCR from pCiES (14), kindly provided by David W. Russell. To generate FVenv, an N-terminal FLAG tag (DYKDDDK) and a V5 tag (GKPIPNPLLGLDST) upstream of the C-terminal endoplasmic reticulum (ER) retention signal (KKKNQ) were introduced. The R123A/R126A mutation was introduced by site-directed mutagenesis according to the instructions of Stratagene.[5] All FVenv constructs were cloned into pcDNA3.1/Hygro$^+$ (Invitrogen) and sequenced for verification. Cell lines stably expressing the FVenv variants were generated, selecting for hygromycin resistance as described previously (13). HEK293 cell lines stably overexpressing WT and mutant SPPL proteases have been described (13). The cDNA that encodes SPPL3 is based on GenBank™ RefSeq NM_139015.4. All experiments were performed on poly-L-lysine-coated cell culture dishes. Protease expression was induced for at least 48 h by supplementing the media with 1 μg/ml doxycycline (BD Biosciences). Transient plasmid DNA transfections were carried out using Lipofectamine 2000 (Invitrogen) according to the manufacturer's instructions. Cells were analyzed for protein expression 48 h post-transfection.

siRNA-mediated Knockdown Experiments and TaqMan RT-PCR—siGENOME SMARTpool siRNAs targeting human SPPL3 and SPPL2a and controls were obtained from Dharmacon. Human SPPL2b-specific single oligonucleotides and controls were purchased from Qiagen. siRNAs were transfected using Lipofectamine RNAiMAX (Invitrogen). Cells were analyzed on day 4 or 5 post-transfection. Quantitative TaqMan RT-PCR was used to control knockdown efficiency. Total cellular RNA was isolated using the RNeasy kit and QIAshredder homogenizers (Qiagen). Up to 2 μg of total RNA was reverse-transcribed using a high capacity reverse transcription kit (Applied Biosystems) according to the manufacturer's instructions. Quantitative PCR was performed using predesigned TaqMan probes for human SPPL2a, human SPPL2b, and human β-actin (Applied Biosystems). Signals obtained were normalized to β-actin, and relative mRNA levels were determined by the $\Delta\Delta C_T$ method.

Cell Lysates, (Co)Immunoprecipitation, and Immunoblotting—Cells were harvested on ice and lysed in 150 mM NaCl, 50 mM Tris (pH 7.6), and 2 mM EDTA supplemented with 1% Nonidet P-40, 1% Triton X-100, and protease inhibitor mixture (Sigma-Aldrich). Lysates were either directly analyzed or subjected to immunoprecipitation as indicated in the figures. For co-immunoprecipitation of substrates and proteases, cellular membranes were prepared as described previously (15). Membranes were lysed in 25 mM HEPES-KOH (pH 7.6), 100 mM potassium acetate, 2 mM magnesium acetate, and 1 mM DTT supplemented with 1% CHAPSO (Sigma-Aldrich) on ice. Membrane lysates were subjected to immunoprecipitation as described (16). Electrophoresis and immunoblotting were carried out as described previously (17). Quantification of proteins from Western blots was carried out as described (18).

RESULTS

FVenv Is Proteolytically Processed by SPPL Proteases—FVenv glycoproteins are initially synthesized as type III transmembrane protein precursors and harbor unusually long membrane-tethered signal or leader peptides (Fig. 1*A*) (12). We studied proteolytic Env processing of the human isolate of the chimpanzee foamy virus (SFVcpz(hu)) (19). Post-translationally, the 130-kDa FVenv protein is proteolytically processed at two sites by furin or furin-like proprotein convertases (PCs) (Fig. 1*A*) (20–23). This generates the N-terminal 18-kDa leader peptide (LP18, $gp18^{LP}$), the 80-kDa surface subunit (SU, $gp80^{SU}$), and the C-terminal 48-kDa membrane-anchored subunit (TM, $gp48^{TM}$) (Fig. 1*A*) (12). ER localization of FVenv is mediated by a C-terminal KKKNQ motif (24) and was not affected by the epitope tags that we attached to the FVenv protein (supplemental Fig. S1*A*).

[5] Primer sequences are available upon request.

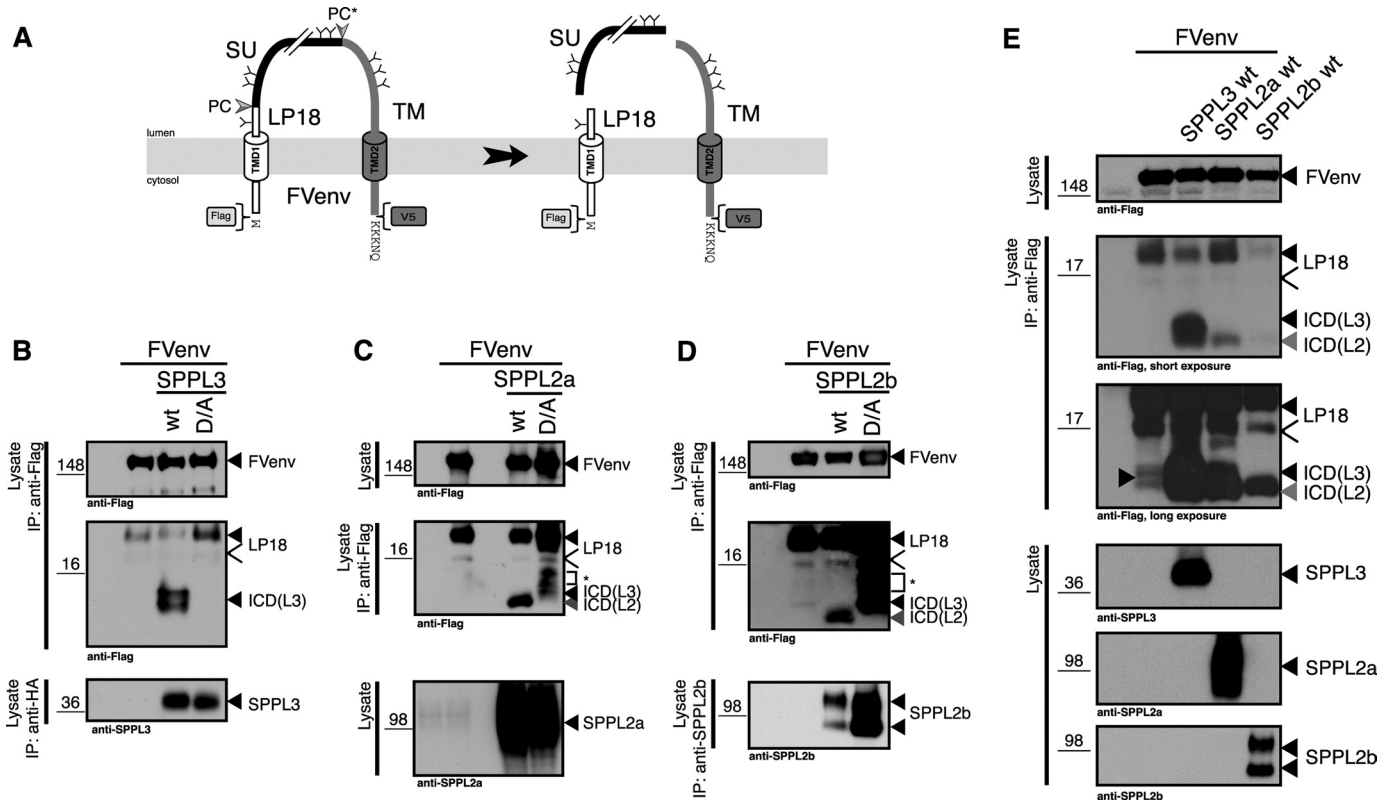

FIGURE 1. **SPPL-mediated proteolysis of FVenv.** *A*, schematic overview of FVenv processing by PCs. The FVenv glycoprotein consists of a leader peptide (LP18), a surface subunit (SU), and C-terminal membrane-spanning domain (TM). PC and PC* cleavage site (*arrowheads*), the C-terminal ER retrieval signal (KKKNQ), and the epitope tags (FLAG and V5) are indicated. Glycosylation sites are also indicated (*Y*). *B–E*, FVenv proteolytic fragments were isolated from HEK293 cells coexpressing FVenv and the indicated SPPL proteases either as catalytically active (WT) or inactive (Asp-to-Ala (*D/A*)) variants. The *open arrowheads* indicate unglycosylated LP18. Coexpression of WT SPPL3 resulted predominantly in generation of ICD(L3) (*black arrowheads*), whereas catalytically active SPPL2a/b produced predominantly ICD(L2) (*gray arrowheads*). Upon coexpression of FVenv and SPPL2a/b Asp-to-Ala mutants, ICD(L3) and protein fragments (marked with *asterisks*) accumulated. Depending on the resolution of the gel system, ICD(L3) was sometimes detected as a doublet. *IP*, immunoprecipitation.

To test whether members of the SPP/SPPL family are capable of processing the type II-oriented LP18, FVenv was coexpressed with either biologically active SPPL (WT) or the corresponding catalytically inactive aspartate-to-alanine mutant. Upon coexpression of WT SPPL3, a low molecular mass intracellular fragment, termed ICD(L3), was detected that was almost completely absent in cells expressing SPPL3(D272A) (Fig. 1*B*). Coexpression of FVenv with SPPL2a also resulted in the generation a low molecular mass intracellular fragment, termed ICD(L2), which was suppressed upon coexpression of the catalytically inactive mutant SPPL2a(D412A) (Fig. 1*C*). Under the latter condition, additional low molecular mass protein fragments, slightly larger than ICD(L2), accumulated (Fig. 1*C*). As demonstrated by siRNA-mediated knockdown of SPPL3, the smallest of these fragments corresponds to ICD(L3) (supplemental Fig. S2), which is generated by endogenous SPPL3 activity. The other protein fragments (labeled with an *asterisk* in Fig. 1, *C* and *D*, and supplemental Fig. S2) remained unchanged upon SPPL3 siRNA treatment and most likely result from degradation of the accumulating LP18 (supplemental Fig. S2). Processing of FVenv by SPPL2b was highly similar to that by SPPL2a (Fig. 1*D*). Expression of SPP induced toxicity in our system; therefore, we were not able to study processing of FVenv by SPP (data not shown). Direct comparison of the ICD species generated by the different SPPL proteases confirmed that ICD(L3) has a slightly different running behavior compared with ICD(L2) (Fig. 1*E*). Processing of FVenv by SPPL2a or SPPL2b predominantly resulted in the generation of ICD(L2), whereas only minor amounts of ICD(L3), probably resulting from endogenous SPPL3 activity, were detected (Fig. 1*E*). Coexpression of SPPL3 and FVenv resulted in massive production of ICD(L3) (Fig. 1*E*) and ICD(L2) (compare with Fig. 4*A*). However, because of the limited resolution of the gel system, we could not fully separate ICD(L3) and ICD(L2) under these conditions. Taken together, these data suggest that FVenv is a substrate for intramembrane proteolysis mediated by SPPL3 and its homologs SPPL2a and SPPL2b, which generate two distinct intracellular fragments of FVenv.

Cleavage of FVenv by SPPL3 Is Independent of Shedding—N-terminal PC cleavage of FVenv separates LP18 and SU/TM (Fig. 2*A*), whereas the more C-terminal PC* cleavage is hardly observed upon cellular expression of FVenv containing the ER retrieval signal (25). Thus, processing of FVenv at the N-terminal PC cleavage site is comparable with a classical shedding event of single-span transmembrane proteins required for subsequent intramembrane proteolysis. To inhibit processing of FVenv by PC, the R123A/R126A mutation (FVenv mut) was introduced (Fig. 2*A*). Subcellular localization of FVenv was not affected by the mutation (supplemental Fig. S1*B*). As expected, processing of FVenv mut by PC was strongly diminished, and

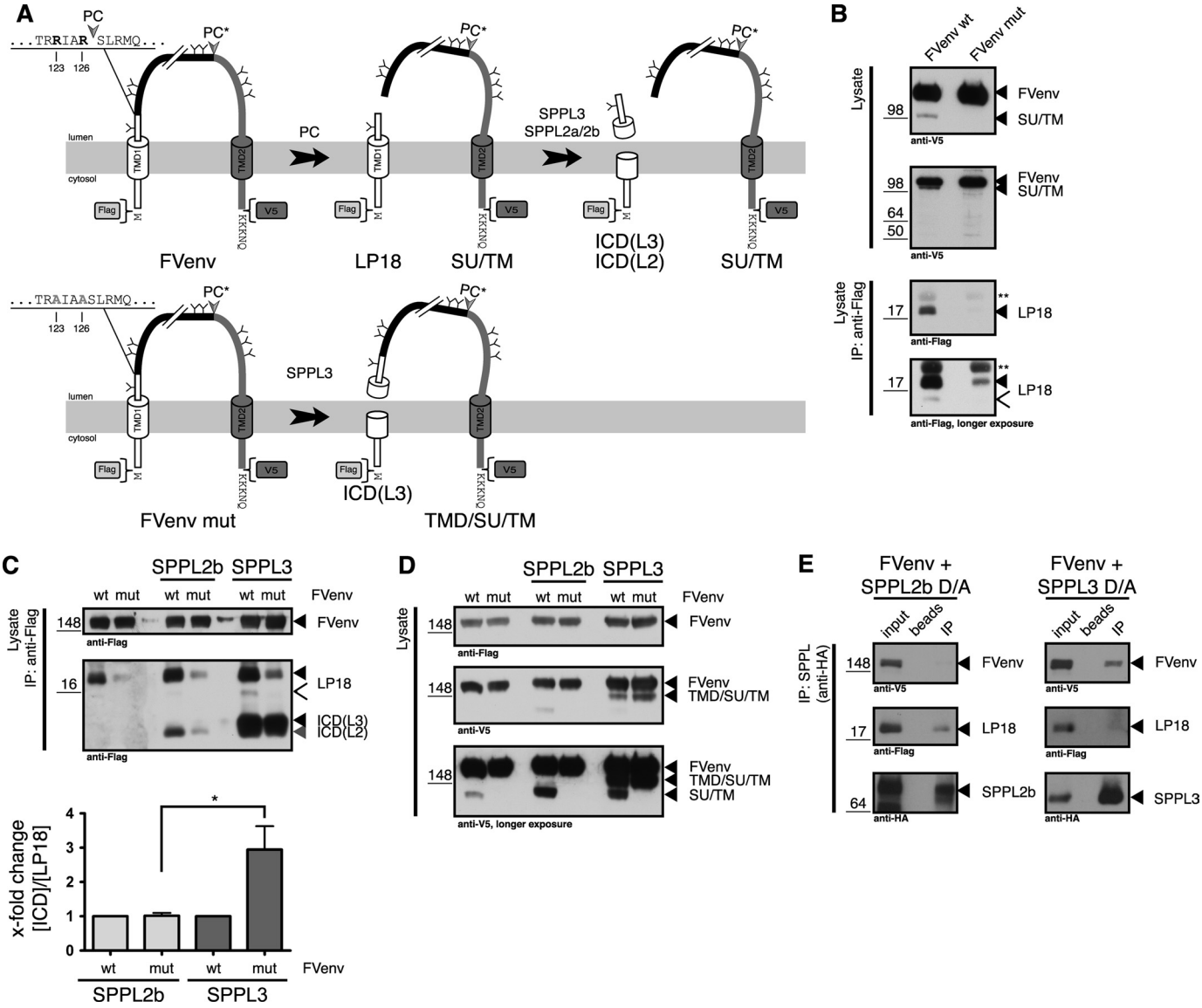

FIGURE 2. **SPPL3 cleavage of FVenv is independent of shedding.** *A*, model depicting the proteolytic processing of FVenv and FVenv mut disregarding the C-terminal PC* cleavage site, which is hardly observed upon cellular expression of FVenv containing the ER retrieval signal. FVenv mut carries a R123A/R126A mutation to abolish cleavage at the N-terminal PC cleavage site. The respective cleavage products are denoted. Amino acids are depicted using the single-letter code. *B*, WT FVenv and FVenv mut were transiently transfected into HEK293 cells, and cleavage products were monitored. Note that processing of FVenv mut by endogenous PC was strongly reduced at the N-terminal PC cleavage site due to the mutation introduced and that, as expected, the C-terminal PC* cleavage site was hardly used at all. The IgG background signal is indicated (**). All other species are labeled as described in the legend to Fig. 1. *C*, WT FVenv or FVenv mut was transiently coexpressed in HEK293 cells stably expressing catalytically active SPPL2b or SPPL3. LP18 and ICD species generated by SPPL are indicated. The quantification depicts ICD levels relative to LP18. Ratios in cells expressing the indicated protease and WT FVenv were set to 1. Data represent means ± S.E. of three independent experiments. *, $p < 0.049$ (Student's unpaired *t* test). *D*, the samples shown in *C* were analyzed for high molecular mass fragments of FVenv. SPPL3-mediated cleavage of FVenv generated ICD(L3) and TMD/SU/TM. Note that TMD/SU/TM was detected exclusively in cells expressing SPPL3. The respective cleavage products in *B* and *C* are indicated according to *A*. *E*, CHAPSO lysates of cellular membranes from HEK293 cells coexpressing the catalytically inactive mutants of the indicated proteases and FVenv were subjected to immunoprecipitation (*IP*) against HA-tagged SPPL2b and SPPL3. Co-isolated FVenv fragments were detected as indicated. To determine the total amount of FVenv present in the lysate, 5% of the total lysate was applied (*input*). To trace unspecific binding, the respective CHAPSO lysates were incubated with protein A-Sepharose beads only (*beads*). Note that SPPL2b(D421A) preferentially co-immunoprecipitated LP18 and only minor amounts of FVenv, whereas SPPL3 selectively co-immunoprecipitated full-length FVenv.

the levels of LP18 and SU/TM were significantly reduced (Fig. 2*B*). Thus, FVenv mut represents a valid model substrate that does not undergo shedding.

Initial shedding is known to be required for SPPL2b-mediated intramembrane proteolysis (10). In line with this, ICD(L2) production correlated with the reduction of LP18 upon coexpression of SPPL2b and FVenv mut (Fig. 2*C*). In contrast, coexpression of SPPL3 with FVenv mut hardly affected ICD(L3) generation, although LP18 was significantly reduced (Fig. 2*C*). Moreover, an additional high molecular mass protein fragment (TMD/SU/TM) that was anti-V5 but not anti-FLAG immunoreactive was detected upon coexpression of FVenv and SPPL3 but not SPPL2b (Fig. 2*D*). Hence, TMD/SU/TM likely originated from intramembrane cleavage by SPPL3. Interestingly, TMD/SU/TM was observed upon SPPL3 overexpression even when FVenv was processed by PC. We therefore conclude that SPPL3 may preferentially cleave full-length FVenv to generate ICD(L3) and TMD/SU/TM, whereas SPPL2b preferentially cleaves LP18.

To address whether generation of ICD(L3) and TMD/SU/TM is a result of direct proteolytic cleavage of FVenv by SPPL3 or is catalyzed by an unknown protease that is activated by SPPL3, we performed co-immunoprecipitation assays using the catalytically inactive variants of SPPL2b and SPPL3. SPPL2b(D421A) predominantly co-isolated with LP18, whereas full-length FVenv was co-isolated only to a minor extent. In contrast, SPPL3(D272A) predominantly co-isolated with full-length FVenv and only to a minor extent with LP18 (Fig. 2*E*), indicating that both enzymes directly interact with the substrate, suggesting that proteolysis of LP18 and FVenv is mediated directly by SPPL2b and SPPL3, respectively. Furthermore, these data strengthen the previous observation that SPPL3 is capable of cleaving FVenv independent of prior processing by PC, whereas SPPL2b requires the short ectodomain of LP18 for efficient cleavage.

Cleavage of FVenv by SPPL3 Is Insensitive to GxGD Protease Inhibitors—To investigate whether G*x*GD protease inhibitors block SPPL-mediated intramembrane proteolysis of FVenv cells coexpressing either WT SPPL2b (Fig. 3*A*) or WT SPPL3 (Fig. 3*B*), FVenv was treated with increasing concentrations of $(Z\text{-}LL)_2$ ketone, L-685,458, or DAPT. Whereas $(Z\text{-}LL)_2$ ketone was shown to target the active site of SPP and SPPL2a/b but not γ-secretase (7, 13, 16, 26), L-685,458 targets γ-secretase, SPP, and SPPL2a/b (13, 16, 27, 28). In contrast, DAPT blocks only γ-secretase activity and fails to block SPP and SPPL2b activity (16, 27, 28). In line with this, treatment of cells expressing WT SPPL2b with $(Z\text{-}LL)_2$ ketone or L-685,458 resulted in a concentration-dependent reduction of ICD(L2) and a simultaneous accumulation of LP18 (Fig. 3*A*). In addition, a concomitant accumulation of ICD(L3) and higher molecular mass protein fragments (Fig. 3*A*), similar to those detected upon coexpression of SPPL2b(D421A) (compare with Fig. 1*D*), was observed. As expected, DAPT had no effect on the processing of LP18 by WT SPPL2b (Fig. 3*A*). Strikingly, none of the inhibitors was capable of reducing the generation of ICD(L3) from cells coexpressing WT SPPL3 and FVenv (Fig. 3*B*). $(Z\text{-}LL)_2$ ketone and L-685,458 even increased the amount of ICD(L3), whereas LP18 levels were hardly affected (Fig. 3*B*). These data demonstrate that cleavage of FVenv by SPPL3 is not inhibited by any of the G*x*GD protease inhibitors tested.

Consecutive Cleavage of FVenv by SPPL3 and SPPL2a/b—To address whether the increased generation of ICD(L3) observed upon treatment with $(Z\text{-}LL)_2$ ketone or L-685,458 (Fig. 3*B*) results from an increased availability of LP18 for SPPL3 cleavage due to inhibition of endogenous SPPL2a/b or from blockage of a subsequent cleavage of ICD(L3) by SPPL2a/b, we optimized our gel system to clearly separate the ICD species generated in cells coexpressing SPPL3 and FVenv (compare with Fig. 1*E*). Separation of the respective samples on a Tris/glycine gel system revealed that generation of ICD(L3) in cells coexpressing SPPL3 and FVenv was accompanied by the generation of a substantial amount of ICD(L2) (Fig. 4*A*). As observed before (Fig. 3*B*), treatment of these cells with L-685,458 or $(Z\text{-}LL)_2$ ketone induced an accumulation of ICD(L3) (Fig. 4*B*) and strongly reduced ICD(L2) generation (Fig. 4*B*). In contrast to L-685,458 and $(Z\text{-}LL)_2$ ketone, treatment with DAPT did not affect the generation of ICD(L3) or ICD(L2) (Fig. 4*B*). TMD/SU/TM, the corresponding SPPL3 cleavage product of FVenv and LP18, was hardly affected by any of the inhibitor treatments (Fig. 4*B*). This again confirms that FVenv cleavage by SPPL3 is insensitive to common G*x*GD protease inhibitors, whereas SPPL2a/b activity is blocked by known SPP/SPPL inhibitors. To confirm that ICD(L2) in this context is generated by endogenous SPPL2a/b, SPPL2a/2b levels were reduced using specific siRNA. Combined knockdown of SPPL2a and SPPL2b caused a selective reduction of ICD(L2), whereas ICD(L3) accumulated (Fig. 4*C*), indicating that ICD(L3) is turned over by SPPL2a/b to a certain extent. LP18 and TMD/SU/TM remained unchanged under these conditions (Fig. 4*C*). In contrast, siRNA-mediated knock-

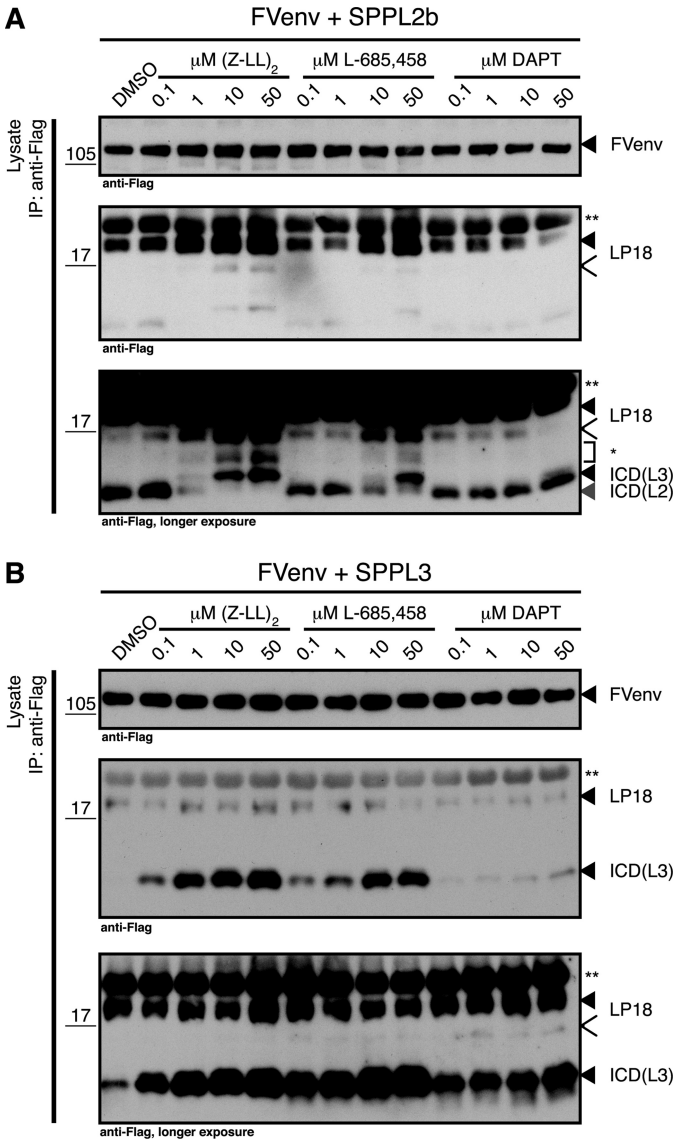

FIGURE 3. **SPPL3 cleavage of FVenv is insensitive to GxGD protease inhibitors.** HEK293 cells stably coexpressing FVenv and catalytically active SPPL2b (*A*) or SPPL3 (*B*) were treated with increasing concentrations of $(Z\text{-}LL)_2$ ketone, L-685,458, or DAPT. FVenv, LP18, and ICD levels were analyzed. Whereas L-685,458 affected ICD production in a similar manner to $(Z\text{-}LL)_2$ ketone, DAPT had no effect on intramembrane proteolysis of FVenv. Note that ICD(L3) generation was not decreased by any of the inhibitors. Upon treatment of cells coexpressing SPPL2b and FVenv, ICD(L3) and protein fragments (*) similar to those detected upon coexpression of SPPL2b(D421A) accumulated (compare with Fig. 1*D*). All species are labeled as described in the legend to Fig. 1. The IgG background signal is indicated (**). *IP*, immunoprecipitation.

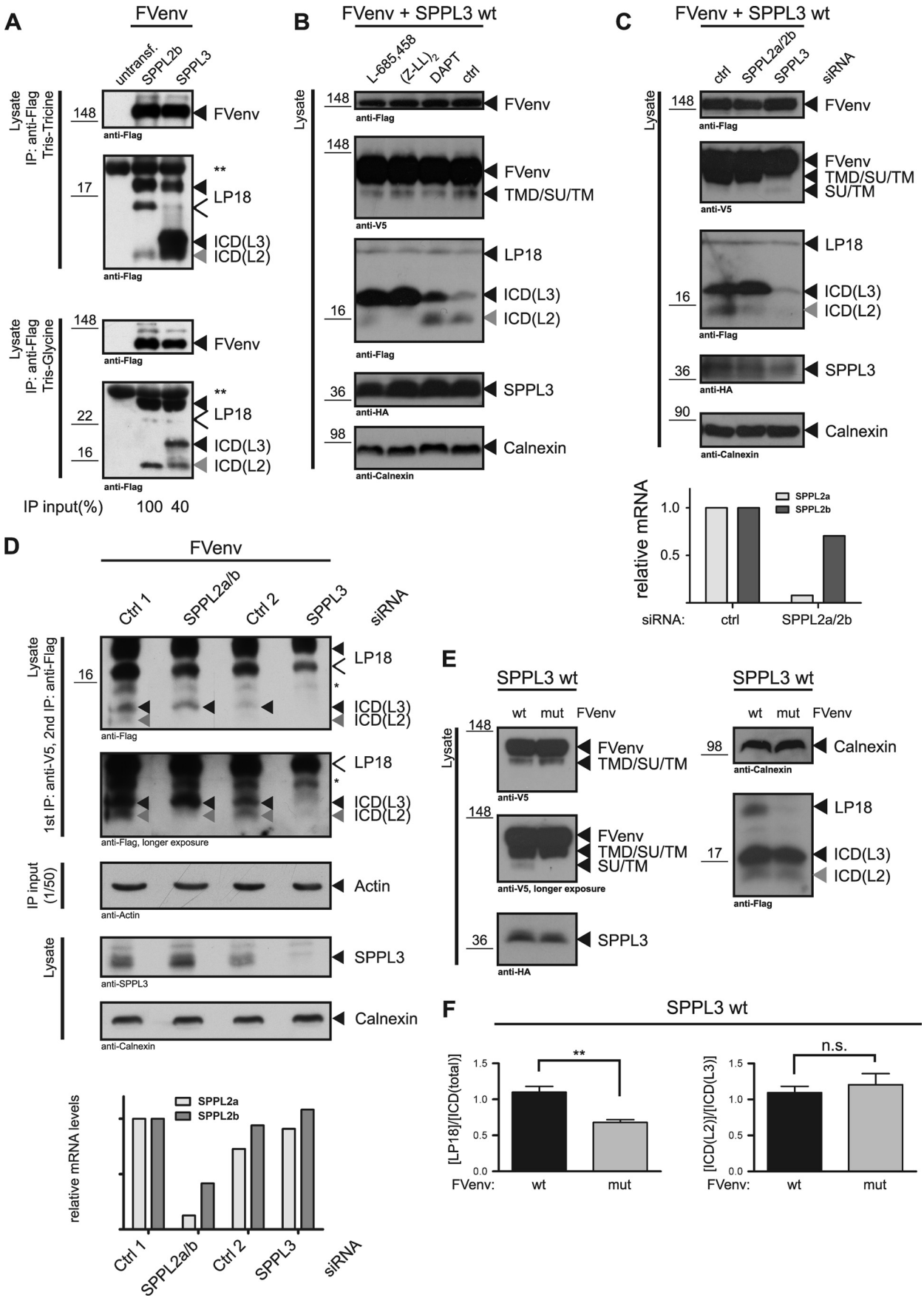
A
FVenv
untransf.
SPPL2b
SPPL3
Lysate
IP: anti-Flag
Tris-Tricine
148
anti-Flag
FVenv
17
**
LP18
ICD(L3)
ICD(L2)
anti-Flag
Lysate
IP: anti-Flag
Tris-Glycine
148
anti-Flag
FVenv
22
16
**
LP18
ICD(L3)
ICD(L2)
anti-Flag
IP input(%) 100 40
B
FVenv + SPPL3 wt
L-685,458
(Z-LL)2
DAPT
ctrl
Lysate
148
anti-Flag
FVenv
148
anti-V5
FVenv
TMD/SU/TM
LP18
16
ICD(L3)
ICD(L2)
anti-Flag
36
anti-HA
SPPL3
98
anti-Calnexin
Calnexin
C
FVenv + SPPL3 wt
ctrl
SPPL2a/2b
SPPL3
siRNA
Lysate
148
anti-Flag
FVenv
anti-V5
FVenv
TMD/SU/TM
SU/TM
LP18
16
ICD(L3)
ICD(L2)
anti-Flag
36
anti-HA
SPPL3
90
anti-Calnexin
Calnexin
relative mRNA
1.0
0.5
SPPL2a
SPPL2b
siRNA:
ctrl
SPPL2a/2b
D
FVenv
Ctrl 1
SPPL2a/b
Ctrl 2
SPPL3
siRNA
Lysate
1st IP: anti-V5, 2nd IP: anti-Flag
16
LP18
*
ICD(L3)
ICD(L2)
anti-Flag
LP18
*
ICD(L3)
ICD(L2)
anti-Flag, longer exposure
IP input
(1/50)
Actin
anti-Actin
Lysate
SPPL3
anti-SPPL3
Calnexin
anti-Calnexin
relative mRNA levels
SPPL2a
SPPL2b
Ctrl 1
SPPL2a/b
Ctrl 2
SPPL3
siRNA
E
SPPL3 wt
wt
mut
FVenv
Lysate
148
FVenv
TMD/SU/TM
anti-V5
148
FVenv
TMD/SU/TM
SU/TM
anti-V5, longer exposure
36
anti-HA
SPPL3
SPPL3 wt
wt
mut
FVenv
98
Calnexin
anti-Calnexin
LP18
17
ICD(L3)
ICD(L2)
anti-Flag
F
SPPL3 wt
[LP18]/[ICD(total)]
1.5
1.0
0.5
0.0
**
FVenv:
wt
mut
[ICD(L2)]/[ICD(L3)]
1.5
1.0
0.5
0.0
n.s.
FVenv:
wt
mut

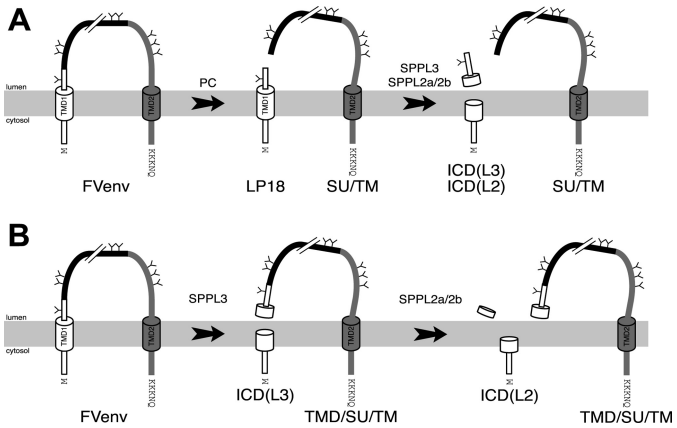

FIGURE 5. **Intramembrane proteolysis of FVenv.** Shown is a schematic overview of proteolytic FVenv processing. Glycosylation sites in FVenv are indicated (*Y*). Proteases and the respective FVenv fragments generated are indicated. FVenv is either processed by SPPL2a/b or SPPL3 following PC cleavage (*A*) or alternatively directly cleaved by SPPL3 and subsequently by SPPL2a/b (*B*).

down of SPPL3, targeting endogenous and overexpressed SPPL3, reduced TMD/SU/TM and both ICD species, whereas LP18 remained unchanged (Fig. 4*C*). A similar observation was made when FVenv processing by endogenous SPPL activity was analyzed (Fig. 4*D*). These data demonstrate that ICD(L2) is generated by endogenous SPPL2a/b. Surprisingly, ICD(L2) generation from cells coexpressing SPPL3 and FVenv was much more efficient than that from cells with reduced SPPL3 activity, although the levels of LP18 were similar, suggesting that ICD(L3) is either turned over more efficiently by SPPL2a/2b than LP18 or is more readily available for SPPL2a/b-mediated cleavage. To ensure that ICD(L2) is directly generated from SPPL2a/b cleavage of ICD(L3) and not by enhanced turnover of LP18, ICD levels in cells coexpressing SPPL3 and either FVenv or FVenv mut (compare with Fig. 2) were compared (Fig. 4, *E* and *F*). Although LP18 levels in cells coexpressing SPPL3 and FVenv mut were significantly reduced by 42 ± 9.0% ($p < 0.004$) compared with FVenv-expressing cells (Fig. 4, *E* and *F*; compare with Fig. 2), the ICD(L2)/ICD(L3) ratio was not significantly affected (Fig. 4, *E* and *F*), excluding that ICD(L2) generation corresponds to the availability of LP18. Taken together, these data suggest that SPPL2a/b is capable of cleaving not only LP18, the PC cleavage product of FVenv, but also ICD(L3), the SPPL3 cleavage product of FVenv. Thus, SPPL3 cleavage of FVenv can serve as an alternative shedding process, generating ICD(L3), which, in addition to furin-generated LP18, serves as a substrate for intramembrane cleavage by SPPL2a/b (Fig. 5).

DISCUSSION

In this study, we have described FVenv as a novel substrate for intramembrane proteolysis by SPPL proteases. In contrast to all SPPL substrates described so far (3), FVenv is cleaved not only by SPPL2a/b but also by SPPL3. In line with previous studies (10), cleavage of FVenv by overexpressed SPPL2a/b is dependent on PC-mediated cleavage, which precedes the intramembrane cleavage and generates LP18, a single-span transmembrane protein with a short ectodomain (Fig. 5*A*). Contrary to our expectations, under the same conditions, SPPL3 is capable of cleaving FVenv also without prior PC-mediated shedding (Fig. 5*B*). Thus, SPPL3 differs from other mammalian intramembrane G*x*GD aspartyl proteases, as it has the ability to cleave substrates without prior shedding under conditions in which SPPL2a/b and presenilin-1/2 strictly depend on shedding. Interestingly, however, rhomboid intramembrane-cleaving serine proteases do not require truncation of their substrate prior to intramembrane proteolysis but cleave intact single-span transmembrane proteins, leading to release of large, soluble, and bioactive factors (29). Hence, in this regard, SPPL3 acts like the members of the rhomboid family and unlike its homologs among the G*x*GD aspartyl proteases. In addition, SPPL3 cleavage of FVenv is the first example of an intact type III transmembrane protein processed by an intramembrane protease because, so far, only single-span transmembrane proteins or polytopic transmembrane proteins, which are converted into single-span transmembrane proteins by an independent proteolytic cleavage, have been shown to undergo intramembrane cleavage by G*x*GD proteases (2, 3, 30, 31).

Because FVenv cleavage by SPPL3 is not reduced by G*x*GD protease inhibitors such as $(Z\text{-}LL)_2$ ketone, L-685,458, and DAPT, our results suggest that SPPL3 displays characteristics distinct from other human G*x*GD proteases. In contrast to our findings, *in vitro* experiments with recombinant *Drosophila melanogaster* SPPL3 and synthetic peptides based on the bovine preprolactin signal sequence (a putative SPP substrate) (32) and cellular assays combining overexpressed human SPPL3 and a model substrate optimized for SPP cleavage (11) demonstrated that SPPL3 may be inhibited by $(Z\text{-}LL)_2$ ketone and L-685,458. However, the findings by Narayanan *et al.* (32) were recently challenged (33), suggesting that such artificial substrates may not be suitable to study the properties of an intramembrane-cleaving protease. The discrepancies regarding the effects of G*x*GD protease inhibitors on SPPL3 may also be explained by substrate- and species-specific effects, as well as

FIGURE 4. **SPPL3 generates a substrate for consecutive SPPL2a/b cleavage.** *A*, HEK293 cells stably coexpressing WT SPPL2b or WT SPPL3 and FVenv were immunoprecipitated (*IP*) using anti-FLAG antibody and separated on a Tris/Tricine gel, as in the previous figures (*upper panels*), or on a Tris/glycine gel (*lower panels*). Note that despite less starting material for the immunoprecipitation (*IP input*), a significant amount of ICD(L2) was generated from cells coexpressing SPPL3 and FVenv. The IgG background signal is indicated (**). *untransf.*, untransfected. *B*, HEK293 cells stably coexpressing WT SPPL3 and FVenv were treated with the indicated inhibitors (10 μM) or the respective carrier (control (*ctrl.*)) for 16 h, and generation of ICD(L3) and ICD(L2) was analyzed in cell lysates. *C*, endogenous SPPL levels of cells described for *B* were reduced by siRNA as indicated, and ICD(L3) and ICD(L2) levels were assessed as described for *B*. Knockdown efficiency was verified by Western blotting (SPPL3) or TaqMan RT-PCR (SPPL2a/b, normalized to actin mRNA levels). *D*, HEK293 cells stably transfected with FVenv were transiently transfected with siRNAs targeting SPPL2a and SPPL2b or SPPL3 (10 nM) or the respective controls (*Ctrl 1* and *Ctrl 2*). Knockdown efficiency was assessed by immunoblotting (SPPL3) or TaqMan RT-PCR (SPPL2a/b). ICD levels were determined by anti-FLAG immunoprecipitation following clearance of FVenv by anti-V5 immunoprecipitation. The *asterisk* indicated the degradation product of LP18 (see supplemental Fig. S2). *E*, cell lysates of HEK293 cells coexpressing SPPL3 and either FVenv or FVenv mut (compare with Fig. 2) were analyzed with regard to the indicated FVenv species. Note that ICD(L2) levels remained unchanged, although LP18 was strongly reduced. *F*, quantification of the experiment shown in *D*. Data represent means ± S.E. of three independent experiments. **, $p < 0.004$ (Student's unpaired *t* test); *n.s.*, not significant. All species are labeled as described in the legend to Fig. 1.

the different context applied in the individual studies. This hypothesis is supported by the observation that a reporter construct based on a signal sequence that is not cleaved by SPP *in vitro* (9) is cleaved by SPP in a cellular context (34). Therefore, additional studies of various enzyme-substrate combinations will be needed to address the issue of whether SPPL3 activity in general is insensitive to common G*x*GD protease inhibitors or only in context with the substrate FVenv.

In accordance with previous studies (10, 35), SPPL2a and SPPL2b only accept FVenv species with a type II membrane orientation and a truncated luminal domain as their substrates. Both LP18 generated by PC cleavage of FVenv and ICD(L3) generated by SPPL3 cleavage of FVenv fulfill this criteria and are cleaved by SPPL2a/b to generate ICD(L2) (Fig. 5). Because ICD(L2) generation by endogenous SPPL2a/b is greatly facilitated when substantial amounts of ICD(L3) are present, our results suggest that ICD(L3) is much more efficiently subjected to subsequent intramembrane cleavage by endogenous SPPL2a/2b than LP18. Given its molecular mass, it is very likely that the luminal domain of ICD(L3) is significantly shorter than that of LP18. Therefore, our results are in line with the previous observation that SPPL2b most efficiently cleaves Bri2 substrates with an ectodomain shorter than 23 amino acids (10). We cannot, however, completely rule out that, for example, different subcellular localizations of LP18 and ICD(L3) favor a more efficient turnover of the latter by SPPL2a/2b.

In contrast to other human G*x*GD proteases, SPPL3 accepts not only LP18 but also the full-length FVenv protein as substrate and, at the same time, generates a product that is an excellent substrate for subsequent intramembrane proteolysis by SPPL2a/b. We therefore conclude that SPPL3 has the ability to serve as an additional sheddase in regulated intramembrane proteolysis of FVenv (Fig. 5*B*). However, whether cleavage of full-length FVenv by SPPL3 also occurs under physiological conditions remains to be elucidated. In addition, future work should address whether SPPL3-mediated proteolysis of FVenv also impacts on virus particle maturation and/or infectivity.

Because it has been shown that cleavage of TNFα by SPPL2a/b occurs within the hydrophobic core of the TMD (16), SPPL2a/b cleavage of FVenv most likely also takes place within the TMD of LP18. Taking into account that the molecular mass of ICD(L3) is larger than that of ICD(L2) but smaller than that of LP18, which contains only 35 amino acids of the luminal part of FVenv, SPPL3 cleavage of FVenv will most likely take place at the very C-terminal part of the FVenv TMD or in the luminal part of FVenv in close vicinity to its TMD. To exactly determine the cleavage sites of SPPLs in FVenv, analysis of the respective cleavage products will be required. However, although extensively tried, we have been unable so far to detect FVenv-derived ICD and C-peptide species using MALDI-TOF-MS (data not shown).

Our study on the intramembrane proteolysis of FVenv indicates that SPPL3 has certain biochemical properties that, based on the current knowledge, were not expected for intramembrane aspartyl proteases of the G*x*GD type but rather for members of the rhomboid family. Future studies will need to address whether this alternative, SPPL3-initiated regulated intramembrane proteolysis pathway is also observed for other physiological substrates of SPPL3 and whether SPPL3 activity itself is regulated.

REFERENCES

1. Lichtenthaler, S. F., Haass, C., and Steiner, H. (2011) Regulated intramembrane proteolysis–lessons from amyloid precursor protein processing. *J. Neurochem.* **117,** 779–796
2. Steiner, H., Fluhrer, R., and Haass, C. (2008) Intramembrane proteolysis by γ-secretase. *J. Biol. Chem.* **283,** 29627–29631
3. Fluhrer, R., Steiner, H., and Haass, C. (2009) Intramembrane proteolysis by signal peptide peptidases: a comparative discussion of G*X*GD-type aspartyl proteases. *J. Biol. Chem.* **284,** 13975–13979
4. Wolfe, M. S. (2009) Intramembrane-cleaving proteases. *J. Biol. Chem.* **284,** 13969–13973
5. Freeman, M. (2008) Rhomboid proteases and their biological functions. *Annu. Rev. Genet.* **42,** 191–210
6. Steiner, H., Kostka, M., Romig, H., Basset, G., Pesold, B., Hardy, J., Capell, A., Meyn, L., Grim, M. L., Baumeister, R., Fechteler, K., and Haass, C. (2000) Glycine 384 is required for presenilin-1 function and is conserved in bacterial polytopic aspartyl proteases. *Nat. Cell Biol.* **2,** 848–851
7. Weihofen, A., Binns, K., Lemberg, M. K., Ashman, K., and Martoglio, B. (2002) Identification of signal peptide peptidase, a presenilin-type aspartic protease. *Science* **296,** 2215–2218
8. Struhl, G., and Adachi, A. (2000) Requirements for presenilin-dependent cleavage of Notch and other transmembrane proteins. *Mol. Cell* **6,** 625–636
9. Lemberg, M. K., and Martoglio, B. (2002) Requirements for signal peptide peptidase-catalyzed intramembrane proteolysis. *Mol. Cell* **10,** 735–744
10. Martin, L., Fluhrer, R., and Haass, C. (2009) Substrate requirements for SPPL2b-dependent regulated intramembrane proteolysis. *J. Biol. Chem.* **284,** 5662–5670
11. Nyborg, A. C., Ladd, T. B., Jansen, K., Kukar, T., and Golde, T. E. (2006) Intramembrane proteolytic cleavage by human signal peptide peptidase-like 3 and malaria signal peptide peptidase. *FASEB J.* **20,** 1671–1679
12. Lindemann, D., and Rethwilm, A. (2011) Foamy virus biology and its application for vector development. *Viruses* **3,** 561–585
13. Martin, L., Fluhrer, R., Reiss, K., Kremmer, E., Saftig, P., and Haass, C. (2008) Regulated intramembrane proteolysis of Bri2 (Itm2b) by ADAM10 and SPPL2a/SPPL2b. *J. Biol. Chem.* **283,** 1644–1652
14. Trobridge, G., Josephson, N., Vassilopoulos, G., Mac, J., and Russell, D. W. (2002) Improved foamy virus vectors with minimal viral sequences. *Mol. Ther.* **6,** 321–328
15. Edbauer, D., Winkler, E., Regula, J. T., Pesold, B., Steiner, H., and Haass, C. (2003) Reconstitution of γ-secretase activity. *Nat. Cell Biol.* **5,** 486–488
16. Fluhrer, R., Grammer, G., Israel, L., Condron, M. M., Haffner, C., Friedmann, E., Böhland, C., Imhof, A., Martoglio, B., Teplow, D. B., and Haass, C. (2006) A γ-secretase-like intramembrane cleavage of TNFα by the G*x*GD aspartyl protease SPPL2b. *Nat. Cell Biol.* **8,** 894–896
17. Fluhrer, R., Capell, A., Westmeyer, G., Willem, M., Hartung, B., Condron, M. M., Teplow, D. B., Haass, C., and Walter, J. (2002) A non-amyloidogenic function of BACE-2 in the secretory pathway. *J. Neurochem.* **81,** 1011–1020
18. Fluhrer, R., Martin, L., Klier, B., Haug-Kröper, M., Grammer, G., Nuscher, B., and Haass, C. (2012) The α-helical content of the transmembrane domain of the British dementia protein-2 (Bri2) determines its processing by signal peptide peptidase-like 2b (SPPL2b). *J. Biol. Chem.* **287,** 5156–5163
19. Meiering, C. D., and Linial, M. L. (2001) Historical perspective of foamy virus epidemiology and infection. *Clin. Microbiol. Rev.* **14,** 165–176
20. Lindemann, D., Pietschmann, T., Picard-Maureau, M., Berg, A., Heinkelein, M., Thurow, J., Knaus, P., Zentgraf, H., and Rethwilm, A. (2001) A particle-associated glycoprotein signal peptide essential for virus maturation and infectivity. *J. Virol.* **75,** 5762–5771
21. Geiselhart, V., Schwantes, A., Bastone, P., Frech, M., and Löchelt, M. (2003) Features of the Env leader protein and the N-terminal Gag domain of feline foamy virus important for virus morphogenesis. *Virology* **310,** 235–244

22. Duda, A., Stange, A., Lüftenegger, D., Stanke, N., Westphal, D., Pietschmann, T., Eastman, S. W., Linial, M. L., Rethwilm, A., and Lindemann, D. (2004) Prototype foamy virus envelope glycoprotein leader peptide processing is mediated by a furin-like cellular protease, but cleavage is not essential for viral infectivity. *J. Virol.* **78,** 13865–13870
23. Geiselhart, V., Bastone, P., Kempf, T., Schnölzer, M., and Löchelt, M. (2004) Furin-mediated cleavage of the feline foamy virus Env leader protein. *J. Virol.* **78,** 13573–13581
24. Goepfert, P. A., Wang, G., and Mulligan, M. J. (1995) Identification of an ER retrieval signal in a retroviral glycoprotein. *Cell* **82,** 543–544
25. Bansal, A., Shaw, K. L., Edwards, B. H., Goepfert, P. A., and Mulligan, M. J. (2000) Characterization of the R572T point mutant of a putative cleavage site in human foamy virus Env. *J. Virol.* **74,** 2949–2954
26. Friedmann, E., Hauben, E., Maylandt, K., Schleeger, S., Vreugde, S., Lichtenthaler, S. F., Kuhn, P. H., Stauffer, D., Rovelli, G., and Martoglio, B. (2006) SPPL2a and SPPL2b promote intramembrane proteolysis of TNFα in activated dendritic cells to trigger IL-12 production. *Nat. Cell Biol.* **8,** 843–848
27. Shearman, M. S., Beher, D., Clarke, E. E., Lewis, H. D., Harrison, T., Hunt, P., Nadin, A., Smith, A. L., Stevenson, G., and Castro, J. L. (2000) L-685,458, an aspartyl protease transition state mimic, is a potent inhibitor of amyloid β-protein precursor γ-secretase activity. *Biochemistry* **39,** 8698–8704
28. Weihofen, A., Lemberg, M. K., Friedmann, E., Rueeger, H., Schmitz, A., Paganetti, P., Rovelli, G., and Martoglio, B. (2003) Targeting presenilin-type aspartic protease signal peptide peptidase with γ-secretase inhibitors. *J. Biol. Chem.* **278,** 16528–16533
29. Lemberg, M. K., and Freeman, M. (2007) Cutting proteins within lipid bilayers: rhomboid structure and mechanism. *Mol. Cell* **28,** 930–940
30. Chen, G., and Zhang, X. (2010) New insights into S2P signaling cascades: regulation, variation, and conservation. *Protein Sci.* **19,** 2015–2030
31. Freeman, M. (2009) Rhomboids: 7 years of a new protease family. *Semin. Cell Dev. Biol.* **20,** 231–239
32. Narayanan, S., Sato, T., and Wolfe, M. S. (2007) A C-terminal region of signal peptide peptidase defines a functional domain for intramembrane aspartic protease catalysis. *J. Biol. Chem.* **282,** 20172–20179
33. Schrul, B., Kapp, K., Sinning, I., and Dobberstein, B. (2010) Signal peptide peptidase (SPP) assembles with substrates and misfolded membrane proteins into distinct oligomeric complexes. *Biochem. J.* **427,** 523–534
34. Nyborg, A. C., Jansen, K., Ladd, T. B., Fauq, A., and Golde, T. E. (2004) A signal peptide peptidase (SPP) reporter activity assay based on the cleavage of type II membrane protein substrates provides further evidence for an inverted orientation of the SPP active site relative to presenilin. *J. Biol. Chem.* **279,** 43148–43156
35. Friedmann, E., Lemberg, M. K., Weihofen, A., Dev, K. K., Dengler, U., Rovelli, G., and Martoglio, B. (2004) Consensus analysis of signal peptide peptidase and homologous human aspartic proteases reveals opposite topology of catalytic domains compared with presenilins. *J. Biol. Chem.* **279,** 50790–50798